Magnus Effects at High Angles of Attack and Critical Reynolds Numbers

A. Seginer* and M. Ringel†
Technion—Israel Institute of Technology, Haifa, Israel

The Magnus force and moment experienced by a yawed, spinning ogive cylinder were studied experimentally in low-speed and subsonic flows at high angles of attack in the vicinity of the critical Reynolds number. Flowfield visualization aided in describing a flow model that divides the Magnus phenomenon into a subcritical region where reverse Magnus loads are experienced, and a supercritical region where these loads are not encountered. The switching of the direction of the Magnus force is correlated with the structure of the vortex wake. The critical values of the spin rate, angle of attack, and cross-flow Reynolds number that determine the boundary between the subcritical and supercritical regions were found to be interdependent. A better understanding of the Magnus effect is obtained by basing the Magnus coefficients and reduced spin rate on the cross-flow velocity. However, the Magnus phenomena are also strongly dependent on the angle of attack.

Nomenclature

C_m = pitching-moment coefficient relative to the nose, normalized by qSd
C_n = yawing-moment (Magnus-moment) coefficient relative to the nose, normalized by qSd
C_{NOR} = normal-force coefficient normalized by qS
C_Y = side-force (Magnus-force) coefficient normalized by qS
d = body diameter
f = spin frequency, rps
l = model length
M = Mach number
P = reduced spin rate, $=pd/2V_\infty \sin\alpha$
p = spin rate, $=2\pi f$; rad/s
q = freestream dynamic pressure
Re = freestream Reynolds number, $=V_\infty d/\nu$
Re_{cf} = cross-flow Reynolds number, $=V_\infty \sin\alpha\,(d/\nu)$
S = reference area, $=\pi d^2/4$
V = velocity
x_{cp} = center-of-pressure location relative to nose tip
α = angle of attack
ν = kinematic viscosity

Subscripts

cf = cross-flow parameters
∞ = freestream parameters

Introduction

A BODY of revolution spinning around an axis inclined to an oncoming flow experiences a force and moment acting in its lateral plane (i.e., side force and yawing moment). These are named after Magnus, who was the first to describe the lift force acting on a two-dimensional cylinder spinning in a crossflow,[1] because the mechanism that generates them is similar to the two-dimensional one. The existence of Magnus effects and their influence on spinning projectiles, especially on spinning spheres, were known more than a century ago and were taken into account in the design of artillery shells. It was assumed that they were linearly dependent on the angle of attack and spin rate.

With the rapid development of modern firearms and low-drag artillery shells in the 1940s and 1950s, the growing data base for various shapes of projectiles and research models brought to light the highly nonlinear variation of the Magnus effects with Mach number, Reynolds number, angle of attack, and spin rate.[2,3] The nonlinear character of the Magnus phenomenon, together with the realization of its important effect on the dynamic stability of spinning projectiles,[4-6] intensified the experimental investigation of this complicated subject.

Initially most of the experiments were conducted on specific projectiles and at the supersonic speeds at which these projectiles were actually flying. However, it was realized earlier[2,7] that the understanding of the basic mechanism of the Magnus phenomenon required measurements on a simple, basic model (the ogive-cylinder spinner was accepted as the standard model), and at low speeds where the data and observed flow mechanisms could be compared with the better known and understood low-speed, two-dimensional Magnus data and with Martin's incompressible theory[8] that was the only existing one at the time.

A systematic, parametric investigation of the effects of the angle of attack, spin rate, and Reynolds number on the basic spinner model at low speeds was conducted by Fletcher.[9] The Reynolds number in this work was based on the model length and was varied by changing the length of the model, however, the cross-flow Reynolds number (at a given angle of attack) remained constant throughout because both the freestream unit Reynolds number and the model diameter were unchanged. Fletcher was the first to report negative Magnus forces (i.e., opposing the classical direction as defined by Magnus) on inclined, spinning bodies of revolution.[9] These forces have been recorded by Fletcher at low reduced spin rates ($pd/2V_\infty$) and at subcritical cross-flow Reynolds numbers when the angle of attack was larger than 15 deg. Under these conditions, the variation of the Magnus force with the spin rate was nonlinear and reversed again to positive when the spin rate was increased. When the cross-flow Reynolds number was increased to critical or higher values, only positive Magnus forces were measured, but they still were nonlinear with spin rate. At angles of attack of 15 deg or less, Fletcher reported only positive Magnus forces that had linear spin-rate-dependent variations.

Negative Magnus forces on two-dimensional spinning cylinders were reported as early as 1910 (Lafay, cited in Ref. 10), but almost half a century passed before an explanation of

Presented as Paper 83-2145 at the AIAA Atmospheric Flight Mechanics Conference, Gatlinburg, TN, Aug. 15-17 1983; received Oct. 14, 1983; revision received Oct. 29, 1984.

*Professor, Department of Aeronautical Engineering. Member AIAA.
†Staff Engineer.

the mechanism that generated them was given by Krahn[11] and verified experimentally by Swanson.[12] Fletcher[13] successfully extended Tani's analysis of transitional, subcritical, and supercritical flows with laminar separations and turbulent reattachments over a stationary two-dimensional cylinder[14] to spinning two-dimensional cylinders. He also presented a plausible explanation of the negative Magnus forces that acted on spinning cylinders at subcritical Reynolds numbers, as opposed to the critical Reynolds numbers on nonspinning cylinders. However, the application of the same two-dimensional explanation to inclined spinning bodies of revolution, using the impulsively started flow analogy, resulted in the wrong sense of the Magnus force.[13] To correct this sense Fletcher had to add the influence of the asymmetrically shed body vortices (because of the spin) whose positions were strongly affected by the cross-flow Reynolds number, and would change the direction of the force with their changing pattern.

Birtwell et al.[15] reported a different class of reverse Magnus forces at small angles of attack ($\alpha < 5$ deg) and at low reduced spin rates (<0.2) that did not agree with Fletcher's explanation of the Magnus sign reversal. The small angles of attack practically precluded vortex shedding, which was an essential part of Fletcher's model, and the cross-flow Reynolds numbers were probably too low for asymmetric transition. The highest cross-flow Reynolds number at which a reverse Magnus force was observed[15] was about 1×10^4 and even when the spin-induced velocity was added, the effective cross-flow Reynolds number was doubled at the most. The results of Ref. 15 also disagreed with the flow model of Ingram et al.[16] which was developed from flow-visualization tests on ogive-cylinder bodies. This flow model predicted classical Magnus forces at low angles of attack α for any spin rate P when the cross-flow Reynolds number Re_{cf} was low, and reverse Magnus forces when Re_{cf} was high. Reference 16 also stated that at high angles of attack, the flowfield was not as sensitive to the cross-flow Reynolds number as at the low angles of attack and that the spin rate characterized the results. It predicted reverse Magnus forces at low spin rates, and classical Magnus forces at moderate to high spin rates. The low α, low Re_{cf}, and low P results of Ref. 16 were in disagreement with those of Ref. 15, and their low α, high Re_{cf} data disagreed with those of Fletcher.[9] Only their high α results seemed to partially agree with Fletcher's.

In a more recent paper, Zehentner et al.[17] presented still different results. Testing at about the same cross-flow Reynolds number and reduced spin rates as Fletcher,[9] they measured reverse Magnus forces at angles of attack between 4 and 10 deg, whereas in this range Fletcher recorded classical values only and measured reverse Magnus forces at $\alpha \geq 20$ deg. On the other hand, whereas Zehentner et al.[17] did not measure reverse forces at $\alpha \leq 4$ deg, Birtwell et al.[15] did, although at higher cross-flow Reynolds numbers. It is interesting to note that Platou[3] obtained reverse and nonlinear Magnus forces at $\alpha \leq 4$ deg in supersonic free flow simply by rounding the corners of the model base, although the same model but with sharp base corners experienced classical and linear forces only. One must wonder if such small geometrical differences between the models could also be responsible for the differences in the subsonic data.

The results of the above-mentioned investigations are summarized in Table 1. With so many discrepancies in the available data and disagreements between the various flow models, the present authors decided to conduct an extensive experimental investigation of the Magnus force and moment acting on a spinning ogive-cylinder model in low-speed and subsonic flows. An effort was made to cover the widest ranges in angle of attack, spin rate, and Reynolds number. Special emphasis was placed in the data reduction on the cross-flow velocity and Reynolds number because most of the angle-of-attack range can be considered high, and because most of the investigators to date agreed on, at least, one feature of the Magnus phenomenon—that the Magnus force at high angles of attack might be comparable to the Magnus force on a spinning cylinder in a crossflow, at the same cross-flow Reynolds number and spin rate.

Apparatus and Procedure

The experiments were conducted in two wind tunnels. The low Reynolds number tests were carried out in a low-speed wind tunnel at speeds from 8 to 32 m/s and unit Reynolds numbers from 4.45×10^5/m to 1.78×10^6/m. The tests with higher Reynolds numbers were conducted in a transonic wind tunnel at Mach numbers from 0.1 to 0.4 and unit Reynolds numbers from 1.78 to 6.44×10^6/m.

The model was a 7.15-caliber, tangent-ogive-cylinder spinner (Fig. 1) with a 1.65-caliber, circular-arc (of 4.25-caliber radius) ogive nose, and a 5.5-caliber, 45-mm-diam cylindrical body. The body was mounted, via a bearing-supported, free-spinning sleeve, on a highly sensitive and accurate standard six-component, wind-tunnel balance.

The model was accelerated to 30,000 rpm within 20 s by blowing air, that was fed through the hollow sting, through a turbine mounted in the model base (Fig. 1). The spin rate was measured by an optical revolution counter built into the bearing housing. A more complete description of this Magnus system, which is an improved version of an earlier one that was described in Ref. 18, is given in Ref. 19.

The test program was divided into three phases. The first phase of the program was a check-out and validation of the new and improved apparatus. Test conditions were similar to Fletcher's[9] and to those of Ref. 18, and the test results were compared. In the second phase, the model was set at $\alpha = 30$ deg and the wind-tunnel runs were performed at freestream diameter-based Reynolds numbers from 2×10^4 to 2.9×10^5 (the corresponding length-based Reynolds numbers varied between 1.43×10^5 and 2.08×10^6). In the third phase, the freestream, diameter-based Reynolds number was set at $Re_d = 8\times10^4$ ($Re_l = 5.72\times10^5$) with an airspeed of 32 m/s and the angle of attack was varied from 0 to 30 deg with 5 deg in-

Table 1 Conclusions from literature review

Reference	Test conditions: Re_{cf}	P	α, deg	Direction of Magnus force[a]
Fletcher[13]	$<Re_{cr}$	low	>15	$C_Y<0$ nonlinear with P
	$\geq Re_{cr}$	[b]	[b]	$C_Y>0$ nonlinear with P
	[b]	[b]	<15	$C_Y>0$ linear with P
Birtwell et al.[15]	$\leq 1\times10^4$	<0.2	<5	$C_Y<0$
Ingram et al.[16]	low	[b]	low	$C_Y>0$
	high	[b]	low	$C_Y<0$
	[b]	low	high	$C_Y<0$
	[b]	high	high	$C_Y>0$
Zehentner et al[17]	[b]	[b]	$4<\alpha<10$	$C_Y<0$

[a] $C_Y>0$ means a "classical" Magnus force; $C_Y<0$ means a reverse Magnus force.
[b] Result is independent of this test condition.

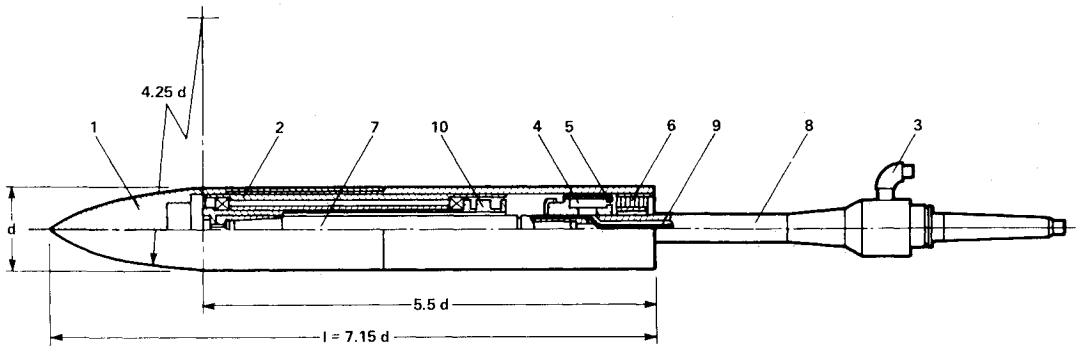

1) MODEL
2) BEARING SYSTEM
3) AIR SUPPLY
4) STAGNATION CHAMBER
5) 4 NOZZLES
6) TURBINE
7) BALANCE
8) STING
9) BALANCE WIRING
10) REVOLUTION COUNTER

Fig. 1 The model and Magnus system.

Table 2 Test conditions

α, deg	$Re_\infty \times 10^{-4}$	$Re_{cf} \times 10^{-4}$	V_∞, m/s	M_∞
30	2	1	8	—
	4	2	16	—
	6	3	24	—
	8	4	32	—
	10	5	—	0.125
	12	6	—	0.150
	14	7	—	0.175
	16	8	—	0.2
	23	11.5	—	0.3
	29	14.5	—	0.4
10	8	1.39	32	0.1
15		2.07		
20		2.74		
25		3.38		
30		4.00		
40		5.14		
50		6.13		
60		6.93		
70		7.52		
80		7.88		
90		8.00		

crements, and from 30 to 90 deg with 10-deg increments. The test conditions are summarized in Table 2.

The model and wind tunnel were set to the predetermined angle of attack and speed/Mach number, respectively, in each test, and the model was spun up to 30,000 rpm. The air supply to the turbine was then turned off to prevent distortion of the Magnus data by an interaction of the turbine exhaust with the flowfield, and the output from the balance and the revolution counter, as well as from the transducers monitoring the wind tunnel performance, was recorded while the spin rate was decaying. The balance and revolution-counter output were reduced to dimensionless coefficients. Forces and moments were reduced to the conventional aerodynamic coefficients using the freestream dynamic pressure, and the body cross-sectional area and body diameter as normalizing area and length, respectively. Moments were referred to the model nose tip. All six of the static aerodynamic coefficients were measured at every data point, including zero-spin conditions, however, this paper presents the Magnus-force and -moment coefficients only.

The conventional, right-hand model coordinate system was used to specify the positive directions of the forces and moments. The x axis coincided with the model longitudinal and spin axis, and was positive pointing upstream. The z axis, normal to the x axis in the pitch plane, was positive pointing downward. The y axis was positive pointing to starboard. With a positive spin (clockwise when facing upstream) the "classical" Magnus force is negative (pointing to port) and the "classical" Magnus moment (referred to the nose) is positive. In the present investigation the model was spinning in the negative direction so that the classical sense of the Magnus force would be positive. This was done to prevent confusion when referring to reverse or negative Magnus forces. With this sign convention and a negative spin, positive side forces ($C_y > 0$) also mean positive or "classical" Magnus forces, and negative side forces ($C_y < 0$) mean negative or "reverse" Magnus forces.

Cross-Flow Velocity as Correlating Parameter

Most of the experiments described herein were conducted at angles of attack that may be considered high ($\alpha > 10$ deg). Investigators agree that, whereas at low angles of attack the Magnus phenomenon may be caused by an interaction of the freestream with the spin-distorted boundary-layer displacement thickness, the mechanism as higher angles of attack is totally different (e.g., Refs. 3, 8, 10, 15, 20-23). It involves the interaction of the freestream with the vorticity shed from the spinning body and can be related to the mechanism that generates the Magnus force on a two-dimensional cylinder

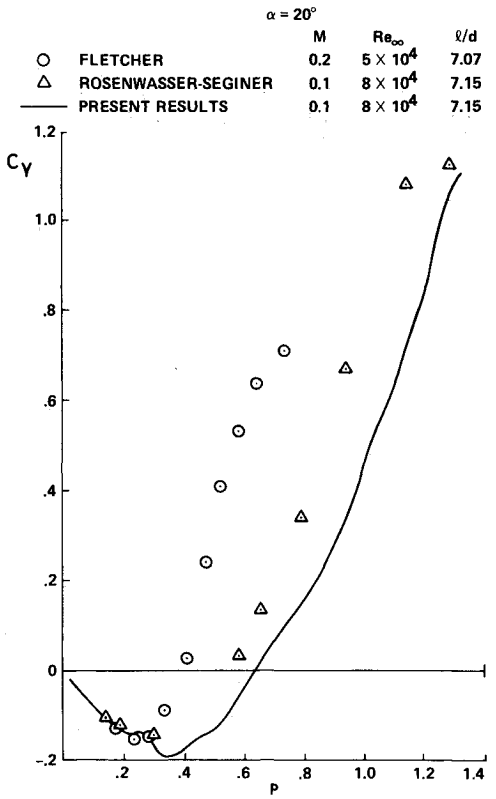

Fig. 2 Comparison of C_Y with existing data.

spinning in a crossflow. This concept led to the attempts to explain the Magnus phenomenon on an inclined, spinning body of revolution by means of an impulsively started, unsteady flow over a spinning, two-dimensional cylinder.[3,13]

If this concept is true, then neither the body-diameter-based freestream Reynolds number nor the body-length-based Reynolds number but, rather, the cross-flow Reynolds number should be the parameter governing the Magnus effects. Therefore, it is presented herein for every data point. Moreover, if the cross-flow mechanism is responsible for the Magnus phenomenon, then the cross-flow velocity ($V_\infty \sin\alpha$) should be a better correlating factor than the conventionally used freestream velocity V_∞. For this reason, and contrary to common practice, the Magnus-force coefficients in this paper have been normalized by the cross-flow dynamic pressure ($q\sin^2\alpha$) and are presented as $C_y/\sin^2\alpha$, and the spin rate has been reduced using the cross-flow velocity to $P = 2\pi fd \div 2V_\infty \sin\alpha$. There was also a practical advantage to this normalization practice that further strengthened its physical justification. It allowed the results of the entire range of angles of attack and Reynolds numbers to be plotted on a common scale and it even collapsed part of the data from tests at different conditions on the same curve.

The cross-flow velocity has been used previously in presenting Magnus results, but never consistently and to such an extent. Platou[3] presented a correlation of the Magnus-force coefficients based on body cross velocity with the cross-flow Mach number M_{cf}. This correlation was good only for $M_{cf} > 0.8$. For lower Mach numbers, Platous's results displayed an unacceptable scatter. Iversen[20] was more successful correlating subsonic Magnus-force coefficients at various angles of attack with a parameter derived from a finite difference solution of a two-dimensional viscous flow over a rotating cylinder and contained the cross-flow velocity. However, this was done for a single freestream Reynolds- and Mach-number combination. Fletcher[13] tried a different correlation parameter based on the impulsive-start flow analogy that included the cross-flow velocity, but succeeded partially at low angles of attack only.

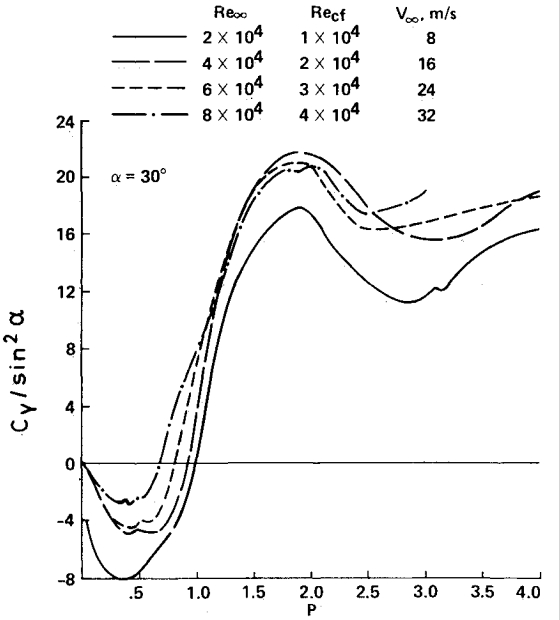

a) $Re_{cf} = 1\times10^4$ to 4×10^4.

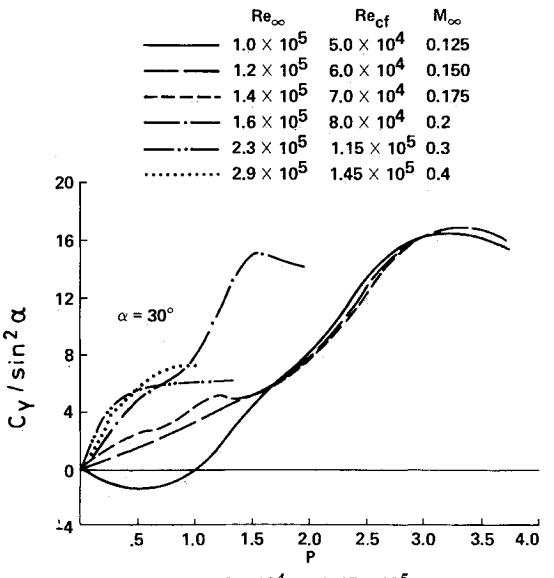

b) $Re_{cf} = 5.0\times10^4$ to 1.45×10^5.

Fig. 3 Effects of Reynolds number on Magnus force, $\alpha = 30$ deg.

Results and Discussion

In the system-validation phase, results were compared with those of Refs. 9 and 18. One example is presented in Fig. 2. The data from all three sources show the same trends, including the reverse Magnus force at low reduced spin rates. The agreement with data obtained previously in the same wind tunnel[18] is good, considering the shortcomings of the older Magnus system. The main difference between Fletcher's data[9] and the present results is in the reduced spin rate at which the Magnus force changes back to the positive direction. It could be attributed to the difference in Reynolds numbers only. Consequently, the next phase of the investigation was a study of the Reynolds number effect on the Magnus phenomenon.

Figure 3 presents the variation of the side-force coefficient with the reduced spin rate at $\alpha = 30$ deg for diameter-based Reynolds numbers from 2×10^4 to 2.9×10^5 (or cross-flow Reynolds numbers from 1×10^4 to 1.45×10^5). The results can be divided into at least three groups. The first group includes the results below $Re_{cf} = 4\times10^4$ (at this cross-flow Reynolds number the boundary layer on a nonspinning cylinder is

laminar, or subcritical). All of the curves in this group show reverse Magnus forces (Fig. 3a). The amplitude of the reverse force is decreasing when the Reynolds number is increased. So also is the reduced spin rate at which the Magnus force turns back to the classical direction. The four curves are qualitatively similar, and the three for $Re_{cf} \times 10^{-4} = 2,3,4$ even merge into a single curve for values of the reduced spin rate of $P > 1.15$. All four curves experience a stall (Magnus "stall") when the reduced spin rate is increased above 1.9, and then recover between $P = 2.5$ and 3.0. When the Reynolds number is increased to $Re_{cf} = 5 \times 10^4$ (or $Re_\infty = 1.0 \times 10^5$, Fig. 3b) the Magnus-force coefficient is still reversed at low spin rates and its amplitude is further reduced, but the sign-reversal spin rate that previously (Fig. 3a) was reduced to $P \cong 0.7$, increases back to $P \cong 1.0$. For Reynolds numbers of $Re_{cf} \geq 6 \times 10^4$ ($Re_\infty \geq 1.2 \times 10^5$) the Magnus force is positive only for this angle of attack ($\alpha = 30$ deg). The second group includes the curves for $Re_{cf} \times 10^{-4} = 5,6,7$ that merge into a single curve for $P > 1.75$ and stall at $P \cong 3.3$. However, the latter two curves are positive for all (measured) spin rates. The third group ($Re_{cf} \times 10^{-5} = 0.8$, 1.15, 1.45), that is also positive everywhere, has a slope higher than the previous group and shows a tendency to stall at much lower spin rates.

Qualitatively, these results agree in part with Fletcher's results for $P < 1.0$ (see Ref. 9, Fig. 7; Fletcher does not present results for higher spin rates), except that his cross-flow Reynolds number is varying because the angle of attack changes. The reduction in both the amplitude and width (on the spin-rate scale) of the reverse Magnus force when the Reynolds number is increased can also be observed in the data of Ref. 17.

In Fig. 3 it is obvious that the variation in the cross-flow Reynolds number, generated by a variation in freestream Reynolds number, strongly affects the Magnus phenomenon. The cross-flow Reynolds number also varies, however, when the angle of attack is changing even for a constant free-stream Reynolds number. The question, will a variation in cross-flow Reynolds number because of a varying angle of attack have the same effect, follows naturally. This question led to the third phase of the investigation, in which the freestream Reynolds number was fixed at $Re_\infty = 8 \times 10^4 (M_\infty = 0.1)$ and the angle of attack was varied between 0 and 90 deg (the $\alpha = 0$ deg data were used only as a reference to ensure the absence of parasite forces, and the $\alpha = 5$ deg data are not presented because of the low signal-to-noise ratio). The Magnus-force-coefficient variation with reduced spin rate is presented in Fig. 4. The angle of attack has a very strong effect on the results. If this is just an angle-of-attack effect, or if it also includes a cross-flow Reynolds number effect, is not immediately obvious. If it does include a Reynolds number effect, it certainly differs from the one just discussed in Fig.3. Although reverse Magnus forces are measured at $\alpha = 10$ and 15 deg, they are quite small and much smaller than those measured at $\alpha = 30$ deg with the same cross-flow Reynolds numbers. These two curves also do not experience a clear stall; they just flatten at $P \cong 1.5$. Being different from the behavior of the Magnus-force curves in Fig.3, this must be a combined angle-of-attack and Reynolds number effect.

The next group of curves includes those for $\alpha = 20$, 25, and 30 deg. They all have reverse Magnus forces with increasing amplitudes as the angle of attack and the cross-flow Reynolds number are increased. In Fig. 3a, an increasing Reynolds number had the opposite effect. The curves in Fig. 4a cross over to the positive side at approximately the same reduced spin rate of $P \cong 0.6$; whereas, in Fig. 3a, the cross-over spin rate was decreasing when the Reynolds number was increased. After becoming positive, the curves have similar slopes but their maximum values before stall, as well as the stall spin rates, are increasing when the angle of attack is increased. The recovery after stall ($P > 2.5$) is quite strong and increasing with the angle of attack.

The curve for $\alpha = 40$ deg (Fig. 4a) leads to the next group of curves (Fig. 4b). The curves for $\alpha = 40$ and 50 deg have the

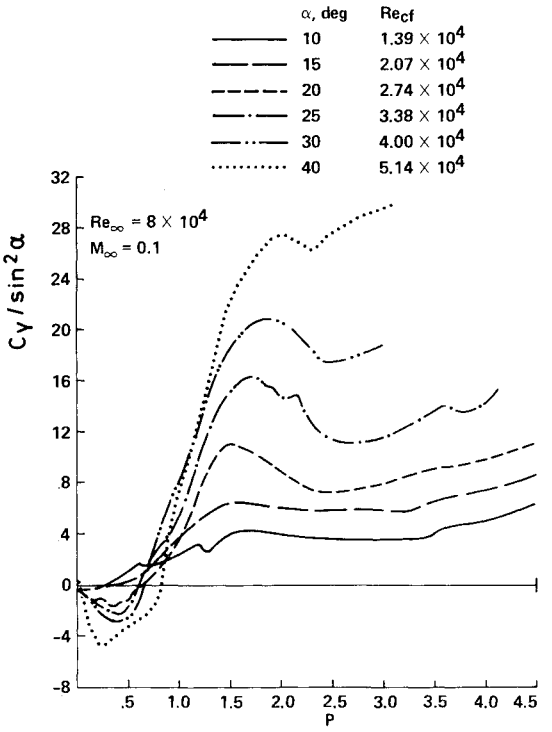

a) 10 deg $\leq \alpha \leq$ 40 deg.

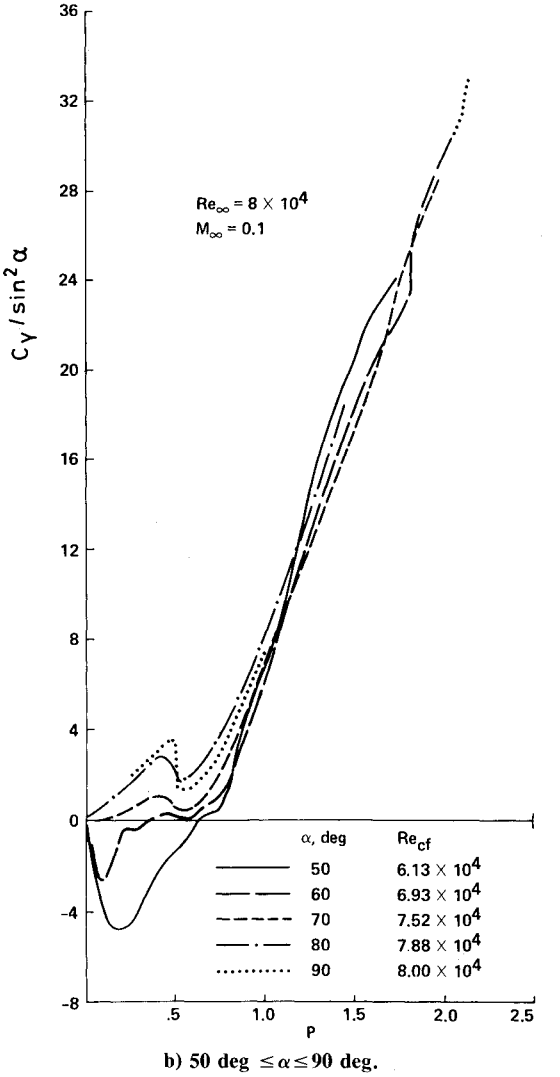

b) 50 deg $\leq \alpha \leq$ 90 deg.

Fig. 4 Effects of angle-of-attack variation on Magnus force, $Re_\infty = 8 \times 10^4$.

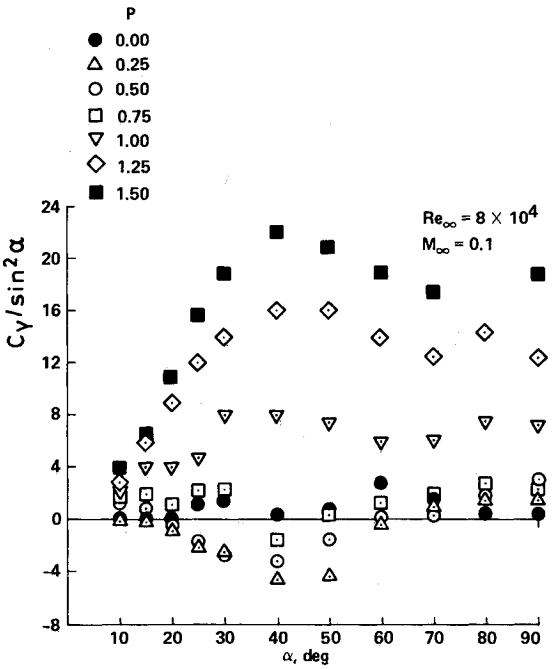

Fig. 5 Magnus-force variation with angle of attack.

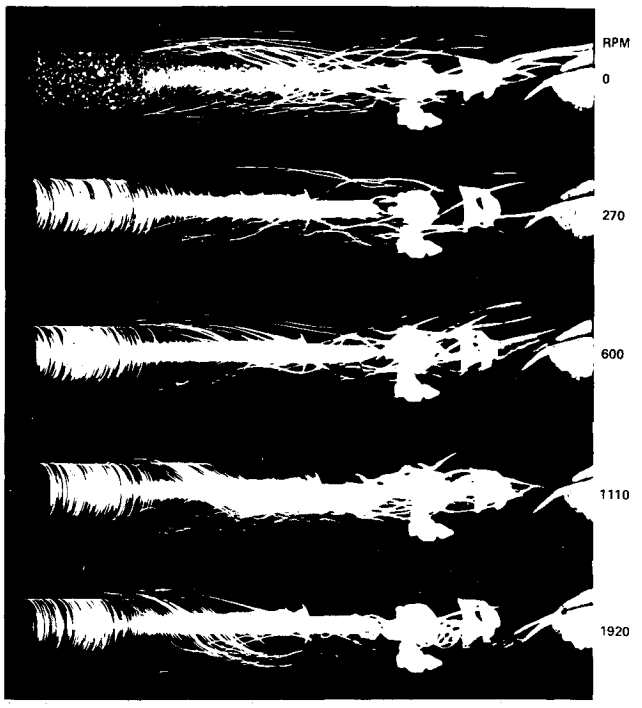

Fig. 6 Helium-bubble visualization of the flowfield; $\alpha = 30$ deg, $Re_\infty = 8 \times 10^4$.

largest negative Magnus-force coefficients. The spin-reversal point suddenly moves to $P \cong 0.85$ for $\alpha = 40$ deg and the slope of the curve increases. For $\alpha > 40$ deg the negative-Magnus-force zone shrinks both in amplitude and width, and above $\alpha = 70$ deg only positive Magnus forces are experienced. The curves for $\alpha \geq 50$ deg have approximately equal slopes (they actually merge) for $P > 1.0$, and stall is not found within the test range of P. There are but small differences, concentrated at low reduced spin rates, between the curves for $\alpha = 70$, 80, and 90 deg. All three curves display a kink at $P \cong 0.55$ that might be a result of a shifting location of the boundary-layer transition line.

Again, only a partial comparison of results with those of Fletcher's is possible. Fletcher found only positive and linear Magnus forces for $\alpha \leq 15$ deg, whereas, in the present work, negative forces were also measured for $\alpha = 10$ and 15 deg. The values of the negative force amplitude, as well as the cross-over values of the reduced spin rate, in Fletcher's results for $\alpha = 20$, 25, and 30 deg also differ from the present results, but one must also bear in mind the differences in cross-flow Reynolds numbers and the strong effect of this parameter (Fig. 3). The Magnus stall observed in the present results cannot be compared with Fletcher's results because his spin rates were not sufficiently high. However, such a stall also was observed, at least qualitatively, by other investigators.[20,24]

Experiments at high angles of attack involve forces and moments in the lateral plane also when the model is not spinning because of asymmetric flow separation and vortex shedding from the body. These effects had to be isolated from the Magnus effects. Figure 5 presents the variation of the Magnus-force coefficient with the angle of attack (with the spin rate as a parameter) that was obtained from the data of Fig. 4 by crossplotting. The Magnus forces are compared with the side force acting on the same, but nonspinning, model. At a reduced spin rate of $P = 1.5$, the Magnus force is an order of magnitude larger than the side force of the nonspinning model. Figure 5 emphasizes the fact that for every angle of attack below 70 deg (at $Re = 8 \times 10^4$) there are spin rates for which the Magnus force is negative; whereas Fig. 4 emphasizes the fact that for spin rates below $P = 0.75$ there are angles of attack for which the Magnus Force reverses its direction.

Judging from all of these results, it can be concluded that the flowfield state at high α can be divided, as far as the flow conditions (i.e., Reynolds number, angle of attack, and spin rate) are concerned, into two categories: a "subcritical" state where reverse Magnus forces can be found (e.g., $\alpha < 70$ deg, $P < 0.75$, and $Re_{cf} < 5 \times 10^4$), and a "supercritical" state where no sign reversal can exist. The boundaries between the two states are not clearly defined, and the limiting value of each one of the above-mentioned parameters depends on the current values of the other two. The helium-bubble visualization presented in Fig. 6 shows the transition from one state to the other. At the lower spin rates, Fig. 6 shows two vortices being shed from the body. In Fig. 6, at f and $P = 0$, the vortices are almost symmetric and are typically those of a nonspinning body. This means that at low angles of attack ($\alpha = 10$ and 15 deg) and very low spin rates ($P < 0.75$), reverse Magnus forces should not be expected or should be very small. This is in agreement with Fig. 5. As the angle of attack is increased (for the same spin rates), asymmetry similar to that on nonspinning bodies can develop and reverse magnus forces can occur (Fig. 5). As the spin rate is increased, the vortex pair begins to be displaced (Fig. 6). A strong asymmetry develops (Fig. 6, at $f = 270$ and 600 rpm) and gradually one vortex disappears (Fig. 6 at $f = 1110$ and 1920 rpm). In the present work, because the model has a negative (counterclockwise looking upstream) rotation, the remaining vortex is swept to port by the spin, with pressures higher in the separated zone on the port side than in the attached high-speed flow on the starboard side of the model, and the Magnus force can act in the classical direction (Fig. 5, high P values for all angles of attack). This mechanism is in qualitative agreement with the flow model of Ref. 16 for high angles of attack, except that, contrary to this model, the present results show that this mechanism works for all of the angles of attack from $\alpha > 10$ deg and upward (Figs. 4 and 5); that at very high angles of attack ($\alpha > 70$ deg) there is no reverse Magnus force at all even when the spin rate is very low (Figs. 4 and 5); and that the cross-flow Reynolds number has a quantitative effect on the mechanism (Fig. 3).

Since the spinning motion induces drastic changes on the flowfield (Fig. 6), including those on the leeward side of the model, one would also expect drastic changes in the force and moment in the pitch plane. Indeed, the two-vortex pattern observed at low spin rates, which is reminiscent of the conventional nonspinning vortex-shedding pattern (Fig. 6, $f = 0$),

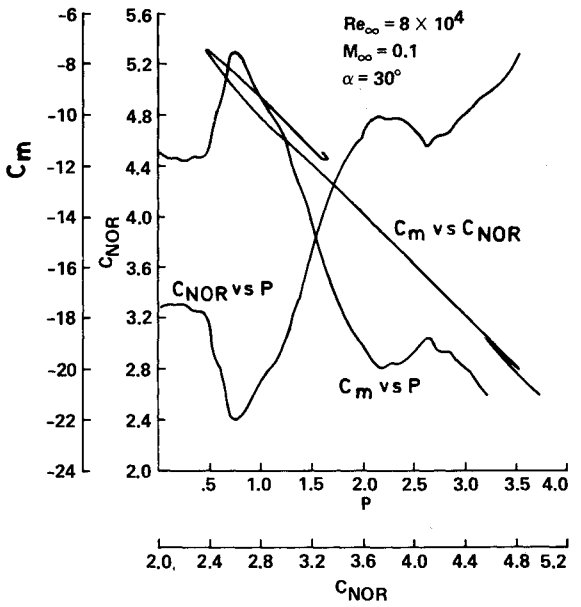

Fig. 7 Normal-force and pitching-moment variations with spin rate.

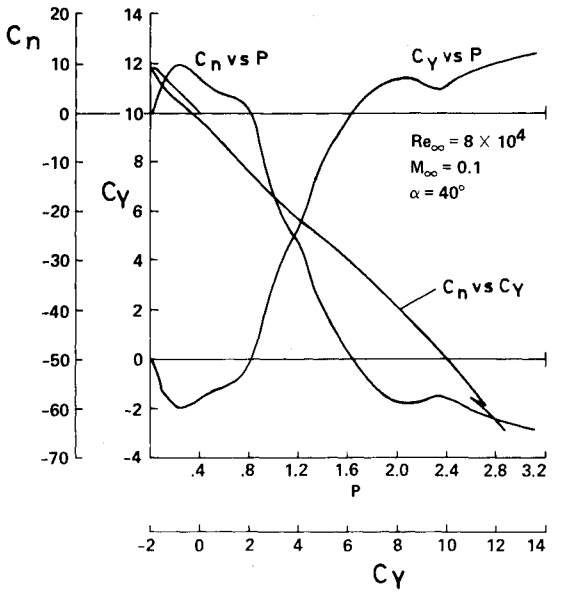

Fig. 8 Magnus-force and -moment variations with spin rate.

generates the expected corresponding normal force and pitching moment associated with the given angle of attack (Fig. 7, $\alpha = 30$ deg at low P). When the spin rate is increased, still in the subcritical region, the normal force begins to decrease. This happens approximately when the magnitude of the reverse Magnus force also begins to decrease (Figs. 7 and 4a, respectively). A further increase in the spin rate past the critical value (in this case, $P \cong 0.75$, see Figs. 4a and 7), changes the Magnus-force direction to positive because the vortex pattern has already been changed drastically (Fig. 6, $f = 1920$ rpm), and the normal force begins to increase because of the increasingly lower pressures induced on the leeward side of the model (Fig. 7). With increasing spin rates, the normal force stalls and then recovers at almost the same spin rates as the Magnus force. The mechanisms of these stalls and recoveries have not been recorded or understood.

It is interesting to note that the variation of the pitching moment with the spin rate is practically a mirror image of the normal-force variation (Fig. 7). This is a surprising result because it means that the location of the longitudinal center of pressure does not change when the spin rate is varying (C_m vs C_N is linear), in spite of the highly nonlinear variation of the normal force with spin rate. This could happen only if the relative axial distribution of the normal force did not change when the spin rate varied, although its local amplitude changed. This is a description of a *two-dimensional* mechanism and because this is the Magnus mechanism it must be also reflected in the lateral, or Magnus, center of pressure. Figure 8 is representative of many such plots that present the variations of the Magnus force and moment with the spin rate and the functional relation between the force and moment. Here too, as in the pitch plane, the moment is a mirror image of the force and the Magnus center of pressure does not move when the spin rate is varying (linear C_n vs C_Y relation in Fig. 8).

Since both centers of pressure are independent of the spin rate, their locations are plotted in Fig. 9 as a function of the angle of attack at a fixed freestream Reynolds number, and as a function of the freestream Reynolds number when the angle of attack is fixed. Both centers of pressure are stronger functions of the angle of attack than of the freestream Reynold number. The different variations with both of these parameters show again, as in Figs. 3 and 4, that the Magnus phenomenon does not depend on the cross-flow Reynolds number only, but has a strong dependence on the angle of attack.

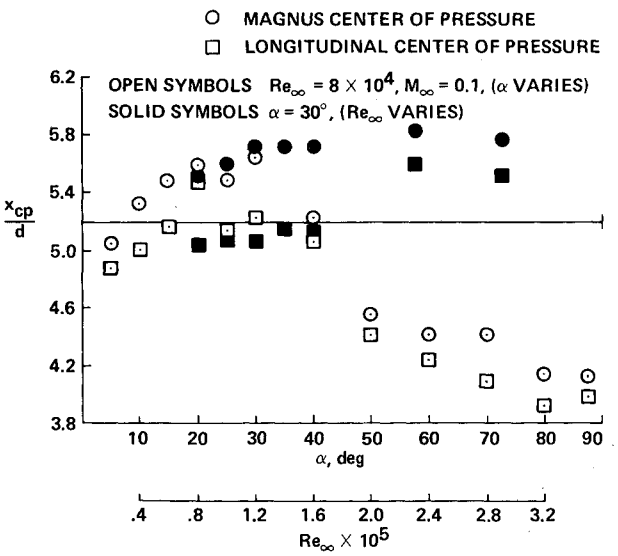

Fig. 9 Longitudinal and Magnus center-of-pressure location variations with angle of attack and Reynolds number.

Conclusions

An extensive experimental investigation of the effects of spin rate, angle of attack, and cross-flow Reynolds number on the Magnus force and moment experienced by a yawed, spinning ogive-cylinder model was conducted in low-speed and subsonic flows. The main conclusions were:

1) The Magnus phenomenon can be divided into two regions, each with a different flow pattern and variation of the aerodynamic coefficients. The subcritical region, at low spin rates below some critical values of angle of attack and Reynolds number, is characterized by reverse Magnus force and moment and a decreasing normal force. In the supercritical region, reverse Magnus loads are not experienced and the normal force is increasing with spin rate.

2) The critical values of the spin rate, angle of attack, and Reynolds number are interdependent. It seems that a three-dimensional critical surface would have to be defined, rather than three separate critical values. Note that the upper limit for the Reynolds number for the reverse-Magnus-phenomenon region is still subcritical in the conventional sense.

3) The Magnus phenomenon is controlled by both the crossflow Reynolds number and the angle of attack. Consequently, its description by the impulsively started two-dimensional flow, that depends on the cross-flow Reynolds number only, cannot be quantitatively complete.

4) The subcritical and supercritical Magnus flowfield states can be related to the structure of the shed vorticity using the helium-bubble visualization technique. The reverse-Magnus-phenomenon region is characterized by two asymmetric vortices, whereas the "classical" Magnus region has only one visible vortex.

5) A Magnus "stall" is experienced by both the Magnus and normal forces. The maximum forces and the stall spin rates depend on the angle of attack and Reynolds number.

6) In spite of highly nonlinear variations of the forces and moments with the spin rate, both longitudinal and lateral centers of pressure remain in a fixed position. This indicates that the Magnus phenomenon is essentially two-dimensional. The locations of the centers of pressure depend, to some degree, on the cross-flow Reynolds number but vary strongly with the angle of attack. This again means that a purely two-dimensional model, such as the impulsively started flow, cannot describe the phenomenon fully.

7) Basing the Magnus coefficients and reduced spin rate on the cross-flow velocity improves the understanding of the flow phenomena.

Acknowledgment

The preparation and presentation of the original AIAA Paper was supported by the National Research Council. The first author was an NRC Senior Research Associate at NASA Ames Research Center during 1982-83.

References

[1]Magnus, F., "Über die Verdichtung der Gase an der Oberfläche glatter Körper," *Poggendorf Annalen der Physikalischen Chemie,* Vol. 88, 1853, pp. 604-610.

[2]Greene, J.E., "A Summary of Experimental Magnus Characteristics of a 7- and 5-Caliber Body of Revolution at Subsonic Through Supersonic Speeds," Naval Ordnance Lab., White Oak, Silver Spring, MD, NAVORD Rept. 6110, Aug. 1958.

[3]Platou, A.S., "Magnus Characteristics of Finned and Nonfinned Projectiles," *AIAA Journal,* Vol. 3, Jan. 1965, pp. 83-90.

[4]Bolz, R.E., "Dynamic Stability of a Missile in Rolling Flight," *Journal of the Aeronautical Sciences,* Vol. 19, June 1952, pp. 395-403.

[5]Murphy, C.H., "Effect of Roll on Dynamic Instability of Symmetric Missiles," *Journal of the Aeronautical Sciences,* Vol. 21, Sept. 1954, pp. 643-644.

[6]Nicolaides, J.D., "Two Nonlinear Problems in the Flight Dynamics of Modern Ballistic Missiles," Institute of Aerospace Sciences, Notre Dame University, Notre Dame, IN, IAS Rept. 59-17, Jan. 1959.

[7]Green, J.E., "Static Stability and Magnus Characteristics of the 5-Caliber and 7-Caliber Army-Navy Spinner Rocket at Low Subsonic Speeds," Naval Ordnance Lab., White Oak, Silver Spring, MD, NAVORD Rept. 3884, Dec. 1954.

[8]Martin, J.C., "On Magnus Effects Caused by the Boundary Layer Displacement Thickness on Bodies of Revolution at Small Angles of Attack," Ballistic Research Lab., Aberdeen Proving Ground, MD, BRL Rept. 870, June 1955; also, *Journal of the Aeronautical Sciences,* Vol. 24, March 1957, pp. 421-429.

[9]Fletcher, C.A.J., "Investigation of the Magnus Characteristics of a Spinning Inclined Ogive-Cylinder Body at $M=0.2$," Weapons Research Establishment, Salisbury, South Australia, TN HSA 159, Oct. 1969.

[10]Kegelman, J.T., Nelson, R.C., and Mueller, T.J., "Boundary Layer and Side Force Characteristics of a Spinning Axisymmetric Body," AIAA Paper 80-1584, Aug. 1980.

[11]Krahn, E., "Negative Magnus Force," *Journal of the Aeronautical Sciences,* Vol. 23, April 1956, pp. 377-378.

[12]Swanson, W.M., "Magnus Effect: A Summary of Investigations to Date," *Journal of Basic Engineering,* Vol. 83, Sept. 1961, pp. 461-470.

[13]Fletcher, C.A.J., "Negative Magnus Forces in the Critical Reynolds Number Regime," *Journal of Aircraft,* Vol. 9, Dec. 1972, pp. 826-834.

[14]Tani, I., "Low-Speed Flows Involving Bubble Separation," *Progress in Aeronautical Science,* Vol. 5, 1965, pp. 70-103.

[15]Birtwell, E.P., Coffin, J.B., Covert, E.E., and Haldeman, C.W., "Reverse Magnus Force on a Magnetically Suspended Ogive Cylinder at Subsonic Speeds," *AIAA Journal,* Vol. 16, Feb. 1978, pp. 111-116.

[16]Ingram, C.W., Lusardi, R.J., and Nicolaides, J.D., "Effects of Rifling and N-Vanes on the Magnus Characteristics of Bodies of Revolution," AIAA Paper 72-970, Sept. 1972.

[17]Zehentner, R.J., Nelson, R.C., and Mueller, T.J., "A Visual Study of the Influence of Nose Bluntness on the Boundary Layer Characteristics of a Spinning Axisymmetric Body," AIAA Paper 81-1901, Aug. 1981.

[18]Rosenwasser, I. and Seginer, A., "The Measurement of Magnus Forces on Spinning Models," *Proceedings of the 23rd Israel Annual Conference on Aviation and Astronautics,* Tel-Aviv and Haifa, Israel, Feb. 1981, pp. 81-88.

[19]Seginer, A. and Ringer, M., "Magnus Effects at High Angles of Attack and Critical Reynolds Numbers," AIAA Paper 83-2145, Aug. 1983.

[20]Iversen, J.D., "Correlation of Magnus Force Data for Slender Spinning Cylinders, "AIAA Paper 72-966, Sept. 1972.

[21]Uselton, J.C. and Carman, J.B., "A Study of the Magnus Effects on a Sounding Rocket at Supersonic Speeds," *Journal of Spacecraft and Rockets,* Vol. 8, Jan. 1971, pp. 28-34.

[22]Sturek, W.B. "Boundary Layer Studies on a Spinning Cone," AIAA Paper 72-967, Sept. 1972.

[23]Vaughn, H.R. and Reis, G.E., "A Magnus Theory," AIAA Paper 73-124, Jan. 1973.

[24]Kahn, D., Oskay, V., and Whiteside, J., "Verification of Ground Test Data by Instrumented Flight Test of an Artillery Shell," AIAA Paper 72-979, Sept. 1972.